CHAPTER 2: Synthesis Procedure and Characterization Details

2.1 Introduction

In the present chapter, the details of synthesis of single phase $Ho_2Ti_2O_7$, $Dy_2Ti_2O_7$ and their doped derivatives by thermochemical solid state reaction method is presented. In this method stoichiometric amounts of the intended precursors are mixed properly and compressed in a pellet before heating in the furnace. In this procedure, final product depends on the time, temperature and heating profile of the thermochemical reaction. In literature, it has been reported that polycrystalline $Ho_2Ti_2O_7$ and $Dy_2Ti_2O_7$ samples were synthesized by solid state thermochemical reaction method in temperature range 1300 ^{0}C to 1500 ^{0}C via intermittent heating and grinding process [67], [68], [98]. The sample synthesis procedure adopted for this thesis work has been detailed in section 2.4. The details of the instruments used and measurement protocol to study the structural, dielectric, magnetic and optical are given in following section.

2.2 Characterization techniques

In the present thesis, synthesized samples are characterized by different experimental techniques to study their physical properties. The basic information and measurement protocol of these techniques are described below.

2.2.1 Powder x-ray diffraction

The powder X-Ray Diffraction method is an analytical technique used to study the structural properties of materials. It provides quick results and non-destructive analysis of the constituting elements without any specific sample preparation. The advantages of the X-ray powder diffraction method are (i) the diffraction pattern obtained from specimen is

characteristic for given element or compound, (ii) the pattern produced by each substance in the mixture is their own and not dependent on others, and (iii) the qualitative and quantitative analysis of the distinct phases present in the mixture is possible. This technique is used to identify and classify the presence of single or multiple crystallographic phases in a material. Moreover, one can also obtained the structural information like- crystal structure, crystal symmetry, lattice constant, atoms position, bond angle and bond length, site-occupancy factors, strain, and many more for as synthesized samples.

For phase purity and structural analysis of the synthesized samples, High-Resolution x-ray diffraction (HRXRD) data has been recorded by using Smart Lab x-ray diffractometer (Rigaku) with Cu $K\alpha_1$ optics near source side. Room temperature HRXRD pattern of all the samples are recorded in 0.7-7.064 $Å^{-1}$ Q range at a step size 0.00071 $Å^{-1}$ (10-120^0 2θ range and step size 0.02^0). For measurements, the powder was obtained from sintered pellets by crushing into fine powder and annealed at 600 °C for 12 h to remove the stresses introduced during crushing. Low temperature powder x-ray diffraction measurements of the samples were performed at P24 beamline in Petra III, DESY, Hamburg, Germany. The synchrotron diffraction pattern was recorded using 25 keV x-ray in 0.7 - 7.3 Q range.

2.2.2 Dielectric measurements

Dielectric spectroscopy has been widely used in the various studies of the relaxation processes occurring in materials. The basic theories dealing with dielectric absorption are well established [99]. The dielectric permittivity (ε) is a frequency dependent quantity representing the characteristic of the medium between two electrodes. Depending on the nature of relaxation and frequency range, one can determine the nature of relaxation in the

dielectric materials. The dielectric permittivity strong depend on the frequency of the externally applied alternating electric field and materials characteristics such as chemical structure, imperfection of the materials, pressure and temperature etc. This makes the dielectric spectroscopy strong tools to study various kinds of disorder in solids. In the present thesis, temperature and frequency dependent complex dielectric behavior has been studied using a Novo control Alpha-A high-frequency analyzer with two different cooling systems (cryogen-free measurement system (CFMS) and closed cycle refrigerator (CCR). For the dielectric measurements, sintered pellets having density ≥ 97%, calculated by the ratio of experimental density (measured by Archimedes's method) and theoretical density, have been used. Before electroding, surface of the sintered pellets was mildly polished using diamond paste and kept in isopropyl alcohol to remove moisture, if any, on the pellet surfaces. Pellets were electroded using silver paste followed by firing at 500 ^{0}C for about 3 minutes. The measurements of all the samples were done in the frequency range of 0.5 Hz-700 kHz and in warming mode having temperature sweep rate 0.5 K/minutes.

2.2.3 SQUID magnetometry

A Superconducting Quantum Interface Device (SQUID) magnetometer has been used to determine the magnetic properties of synthesized samples as a function of temperature, magnetic field and frequency. The high sensitivity of SQUID makes it an ideal instrument for investigation of the magnetic properties of different kinds of materials. Using this instrument one can measure the different magnetic properties such as; time and field dependent magnetization, ac susceptibility, magnetic spin relaxation etc. SQUID Magnetometry require low temperature environment, created by liquid helium, to operate superconducting coil which is also helpful to perform low temperature measurements of the samples. The

magnetometer measures the extremely small change in magnetic flux associated with the movement of sample through superconducting detection coil, which is subsequently converted and measured in the form of current. In the present work, magnetic measurements have been performed by using a Magnetic Properties Measurement System (Quantum Design®, USA). For the magnetic measurements, a small piece of the sintered pellet has been used. Temperature dependent dc magnetization of the samples measured at various field in temperature range 2-300 K with a constant sweep rate 2 K/minutes. The experiments have been performed using standard protocols for zero field cooled warming (ZFCW), field cooled cooling (FCC) and field cooled warming (FCW) measurements. Temperature dependent ac susceptibility of the samples has been measured in ZFCW, FCC, and FCW at different frequency and magnetic field at constant driving ac amplitude 3 Oe and temperature sweep rate 1 K/minute.

2.2.4 UV-Visible spectrophotometer

The UV-Visible spectrometer is used to obtain the absorption spectrum for liquid or solid samples when illuminated by the light in ultraviolet-visible region. The absorbed or reflected wavelength in visible spectral region corresponds to the colour perceived by the material. It is the region in electromagnetic spectrum, where molecules or atoms undergo the corresponding electronic transitions. The dual beam UV–Visible (UV-Vis) spectrophotometer (Hitachi, U-3010) has been used to study the absorption properties of the synthesized samples. The spectrometer measures the ratio of intensity of light after passing through the sample (I) to light intensity before the transmission (I_0). This ratio of intensity (I/I_0) is termed as transmittance (T). The transmittance value obtained using the spectrometer is converted to absorbance using Kubelka-Munk equation given as

$$f(R) = \frac{(1-R)2}{2R} = \frac{k}{s} \quad (2.1)$$

Where, R, k and s represent the absolute reflectance, absorption coefficient and scattering coefficient, respectively [100]. The dual beam spectrophotometer splits the light into two beams before it reaches the sample. One of the beam passes through the sample and the other one is used as reference. The intensity of beam that passes through reference is considered to be 100% transmitted or zero absorbed.

2.2.5 Photoluminescence spectrometer

It is a spectrometer which uses non-destructive and non-contact means to probe about the electronic structure of the materials. It involves a process in which light of certain wavelength is illuminated on the sample which gets absorbed and photo-excitation of material takes place. In this process, the valence band electrons absorb the energy and attain higher electronic states, followed by the permitted transition in the form of photons to acquire a lower energy level. The light emitted during this process is termed as photoluminescence (PL) and the instrument used to study the PL phenomena is termed as photoluminescence spectrometer. The luminescence spectra for the samples involved in the present study has been recorded by use of Hitachi F-4600 Fluorescence spectrometer (Xenon lamp as excitation source).

2.3 Rietveld analysis

In recent years, Rietveld method is most familiar and widely accepted tool for the structural analysis of crystalline materials. In 1967, H. M. Rietveld [101], [102], developed the Rietveld analysis program for the analysis of diffraction pattern of crystalline materials recorded by using x-ray and neutron diffractometers [103]–[105]. In this method, to obtain

the true structure of any crystalline materials, experimental diffraction pattern is fitted by the approximated structural model by using least square method. In the least square approach a theoretical diffraction pattern is generated by the input crystal structure parameters and tried to match with the experimentally observed diffraction pattern of crystalline materials. For the best fit, difference between the theoretical and experimental diffraction pattern is minimized to an acceptable level by adjusting the instrumental and structural refinable parameters. In Rietveld analysis, the quantity used to minimize is χ^2 [105], representing the weighted sum of the squared differences between the observed ($y_{o,i}$) and calculated ($y_{c,i}$) intensity values at the i^{th} step of the diffraction pattern.

$$\chi^2 = \sum w_i.(y_{o,i} - y_{c,i})^2 \qquad (2.2)$$

Where, $w_i = 1/\sigma_{o,i}^2$ and $\sigma_{o,i}^2$ represent the variance of the observed data $y_{o,I}$ [105]–[108]. In the Rietveld analysis various agreement factors are used to determine the quality of fit between experimental and calculated patterns quantitatively. The agreement factor weighted profile R-factor (R_{wp}), reflecting the goodness of fit between calculated and experimental diffraction patterns is square root of the quantity minimized, divided by the weighted intensities [105], [107] defined as

$$(R_{wp})^2 = \sum w_i.\,(y_{o,i} - y_{c,i})^2 \,/\, \sum w_i.\,(y_{o,i})^2 \qquad (2.3)$$

Other agreement factor used in Rietveld fit is expected R-factor **(**R_{exp}). If N is the number of data points, R_{exp} is written as [105], [107]

$$(R_{exp})^2 = N \,/\, \sum w_i.(y_{o,i})^2 \qquad (2.4)$$

From these R-factors χ^2 is defined as

$$\chi^2 = (R_{wp}/R_{exp})^2 \quad (3.5)$$

In the Rietveld fit theoretically the value of χ^2 should be never less than one. However, if fit results in $\chi^2 < 1$ which means that $<(y_{o,i}- y_{c,i})^2>$ is less than $\sigma^2 (y_{o,i})$. This may happen due to the standard uncertainties for the data are overestimated or additional parameters have been introduced so that the model is fitting the noise. Such kinds of features are common in powder diffraction [107]. In the Rietveld analysis different types of profile functions have been recommended to define the peak shape of calculated diffraction pattern. Out of these options Pseudo-Voigt is one of the commonly used functions by the crystallographers. Pseudo-Voigt function (pV(x)) is consists of the linear combination of Lorentzian (L(x)) and Gaussian (G(x)) functions, defined as

$$pV(x)= \eta L(x) + (1- \eta)G(x \quad (3.6)$$

In Rietveld refinement, peak width of the diffraction pattern defined by FWHM (full width at half maximum) is an important variable parameter which depends upon the diffraction angle 2θ in addition to other instrumental factors. FWHM of Gaussian component (H_G) and Lorentzian component (H_L) is modelled by the following equation [109], [110]

$$H_G^2 = U\tan^2\theta + V\tan\theta + W \quad (3.7)$$

$$H_L^2 = X\tan\theta + Y/\cos\theta \quad (3.8)$$

Where, U, V and W are refinable parameters. For specific diffractometer values of U, V and W parameters are considered as fixed unless there is no line broadening from the sample due to particle size and/ or strain. In the present thesis Rietveld refinement of the XRD patterns were carried out by using the FULLPROF SUITE software [110].

2.4 Synthesis of $Ho_2Ti_2O_7$, $Dy_2Ti_2O_7$ and their doped derivatives

To synthesize the Pure phase Polycrystalline sample of $Ho_2Ti_2O_7$ (HTO), $Dy_2Ti_2O_7$ (DTO) and their doped derivatives, high-purity starting powder materials of Ho_2O_3 (≥99.9% assay, Sigma Aldrich), Dy_2O_3 (≥99.9% assay, Alfa Aesar), TiO_2 (≥99.8% assay, Sigma Aldrich), MnO_2 (≥99.9% assay, Alfa Aesar) and Fe_2O_3 (≥99.0% assay, Sigma Aldrich) have been used. Before starting the synthesis procedure, XRD pattern of these raw materials have been recorded to confirm the phase purity of the each material. Figure 2.1 shows the XRD pattern of Ho_2O_3, Dy_2O_3, TiO_2, MnO_2, and Fe_2O_3, confirming the phase purity of raw materials.

To synthesize the samples, raw materials were taken very precisely in stoichiometric proportion and mixed properly using an agate mortar and pestle for 2 hours. Further, these mixtures were homogenized in acetone medium by mechanical ball milling for 8 hours. After homogenization, samples were dried at room temperature. Firing of HTO and its doped derivatives samples was done at 1350 ^{0}C for 20 hours whereas DTO and its doped derivatives were done at 1400 ^{0}C for 20 hours, in alumina crucibles. All the fired samples were crushed into fine powders using a mortar and pestle. Pellets were made using PVA binder which was later burned by heating the samples at 600 ^{0}C for 6 hours. Further, sintering of HTO and its doped derivatives samples was done at 1375 ^{0}C for 20 h whereas DTO and its doped derivatives samples were done at 1450 ^{0}C for 20 h, to obtain the high-density samples. To insure the formation of single phase samples XRD diffraction pattern of all the samples were recorded at room temperature. Figure 2.2 shows the XRD pattern of HTO and its doped derivatives samples whereas figure 2.3 shows the XRD pattern of DTO and its derivatives samples. The HRXRD pattern confirms that all samples are well

crystallize and in single-phase without any extra detectable impurity peaks within the sensitivity limit of the instruments.

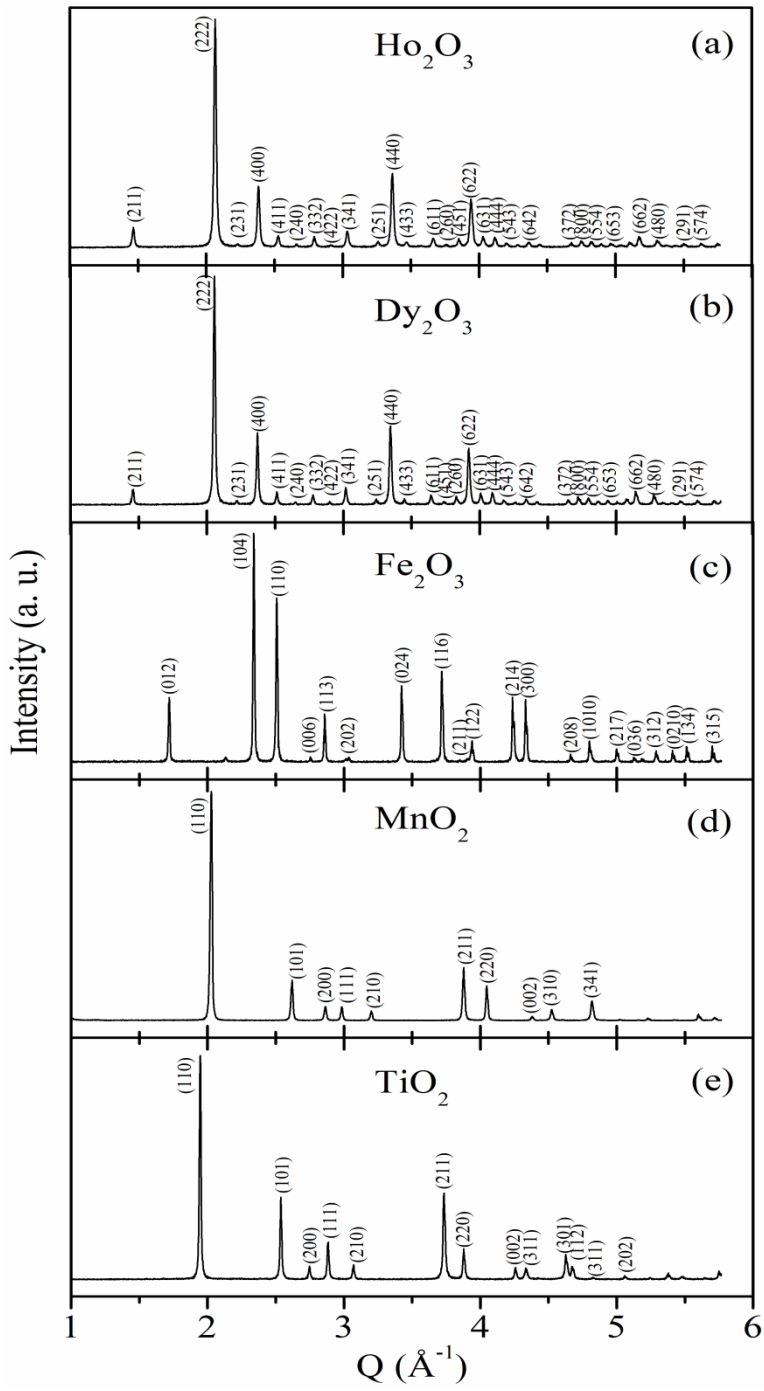

Figure 2.1: x-ray diffraction patterns of the chemicals (a) Ho_2O_3, Dy_2O_3, Fe_2O_3, MnO_2 and TiO_2, used for synthesis of $Ho_2Ti_2O_7$, $Dy_2Ti_2O_7$ and their doped derivatives.

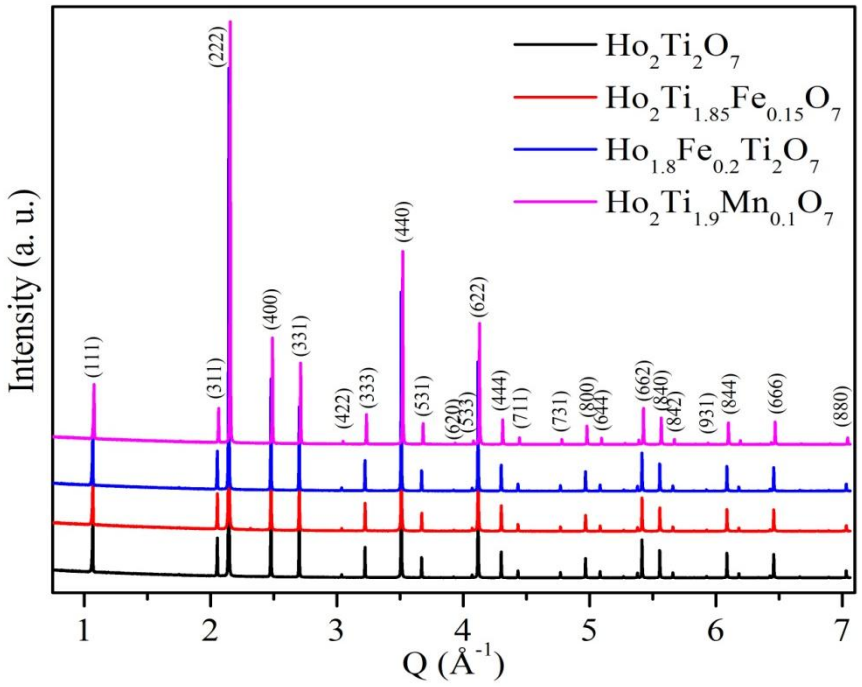

Figure 2.2: Room temperature high-resolution x-ray diffraction pattern of $Ho_2Ti_2O_7$ and its doped derivatives.

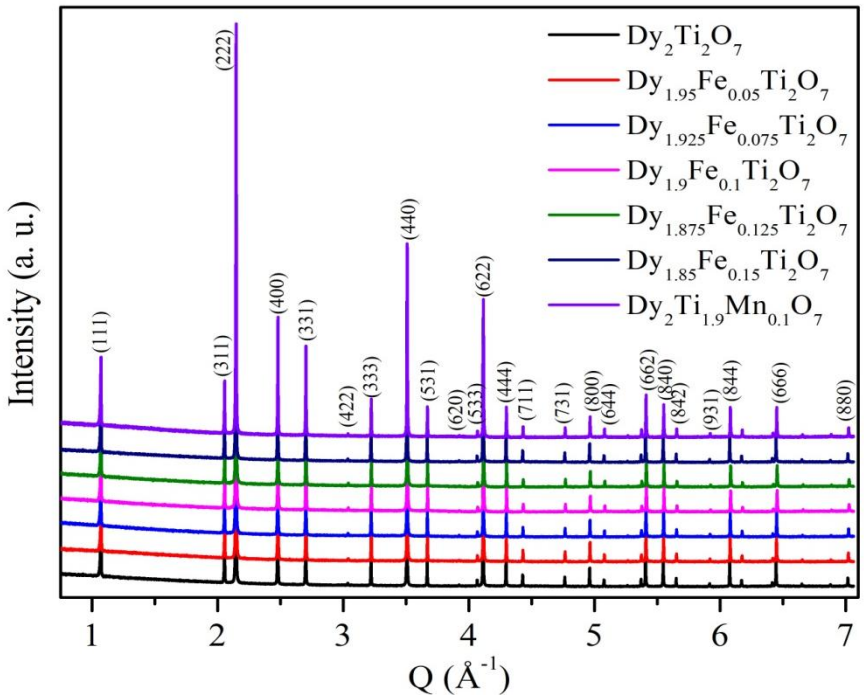

Figure 2.3: Room temperature high-resolution x-ray diffraction pattern of $Dy_2Ti_2O_7$ and its doped derivatives.

Rietveld refinement of the XRD pattern was further used to confirm the position of the atoms and site mixing of HTO, DTO and their doped derivatives samples. According to the crystal structure of HTO and DTO, as discussed in the section 1.5, Ho^{3+}/ Dy^{3+} and Ti^{4+} ions occupy 16d and 16c crystallographic sites, respectively. To confirm the sites of Ho^{3+}/ Dy^{3+} and Ti^{4+} ions, Rietveld refinement of HTO, DTO are performed by considering Ho^{3+}/ Dy^{3+} and Ti^{4+} ions at their crystallographic position as well as switched site position i.e. Ho^{3+}/ Dy^{3+} and Ti^{4+} ions are considered at 16c and 16d crystallographic positions. Figure 2.4 shows the Rietveld fit of HTO for; (a) Ho^{3+} and Ti^{4+} considered at 16d and 16c crystallographic sites, respectively and (b) Ho^{3+} and Ti^{4+} considered at 16c and 16d crystallographic sites, respectively. The obtained values of structural and fitting parameters of HTO are listed in table 2.1. It has been found that on interchanging the site occupancy of Ho and Ti ion from their regular fitting of the XRD pattern gets deteriorated which also reflect in the increment in the χ^2. A similar observation has been observed in case of DTO. The Rietveld fit of the XRD pattern of DTO at their regular position and at off-site occupancy is shown in figure 2.5. Whereas, obtained values of structural and fitting parameters of DTO are listed in table 2.2. These observations confirm the formation of pure phase cubic HTO and DTO having space group $Fd\bar{3}m$ where atoms were situated at the sites intended for.

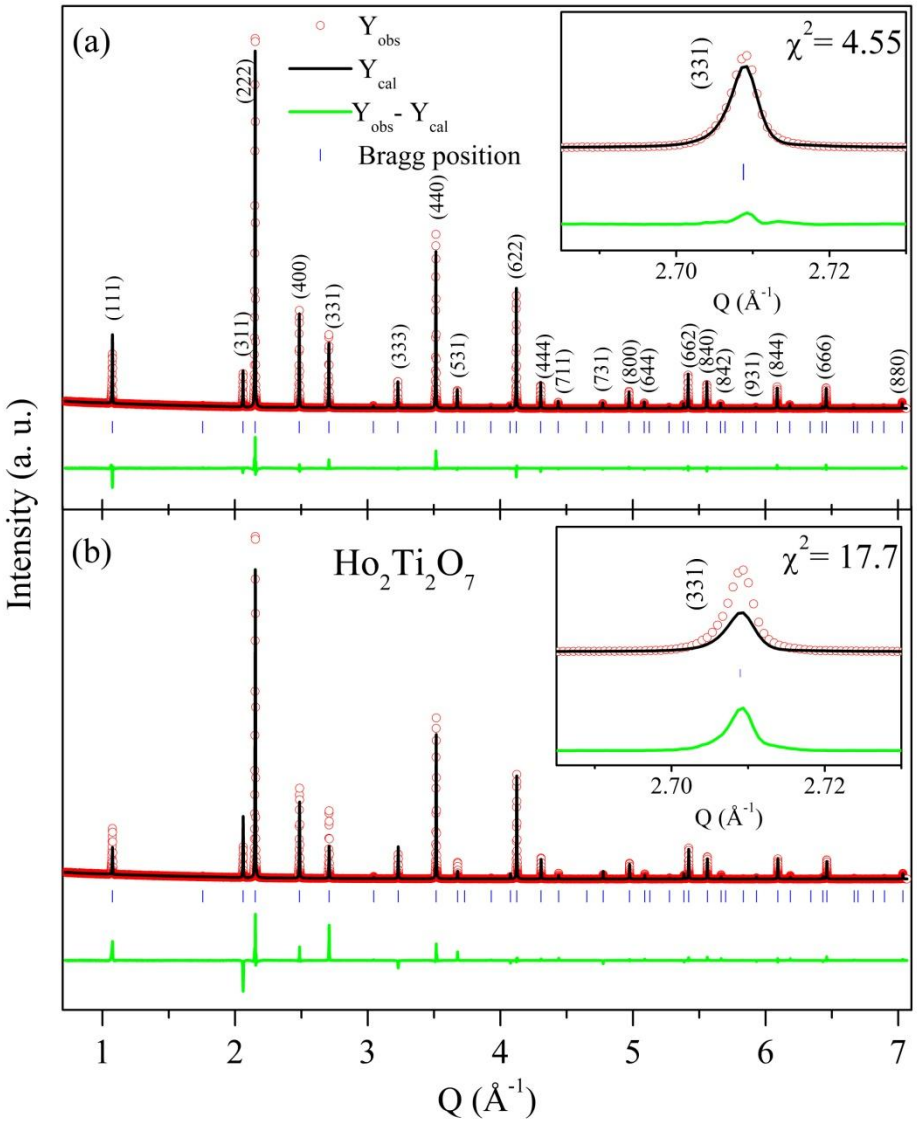

Figure 2.4: Rietveld refinement of the high-resolution x-ray patterns of $Ho_2Ti_2O_7$ by considering; (a) Ho^{3+} and Ti^{4+} at 16d and 16c crystallographic sites, respectively and (b) Ho^{3+} and Ti^{4+} at 16c and 16d crystallographic sites, respectively.

Table 2.1: Details of structural and fitting parameters as obtained from high-resolution x-ray diffraction. Compound, lattice constant, variable coordinate x in the 8f-site, R-factors (R_p, R_{wp} and R_e) and goodness of fit χ^2.

Compound	a (Å)	x (48f)	R_p	R_{wp}	R_e	χ^2
$Ho_2Ti_2O_7$	10.1006(1)	0.324(2)	14.8	14.6	6.86	4.55
$Ti_2Ho_2O_7$	10.1006(1)	0.416(0)	24.0	28.9	6.87	17.4

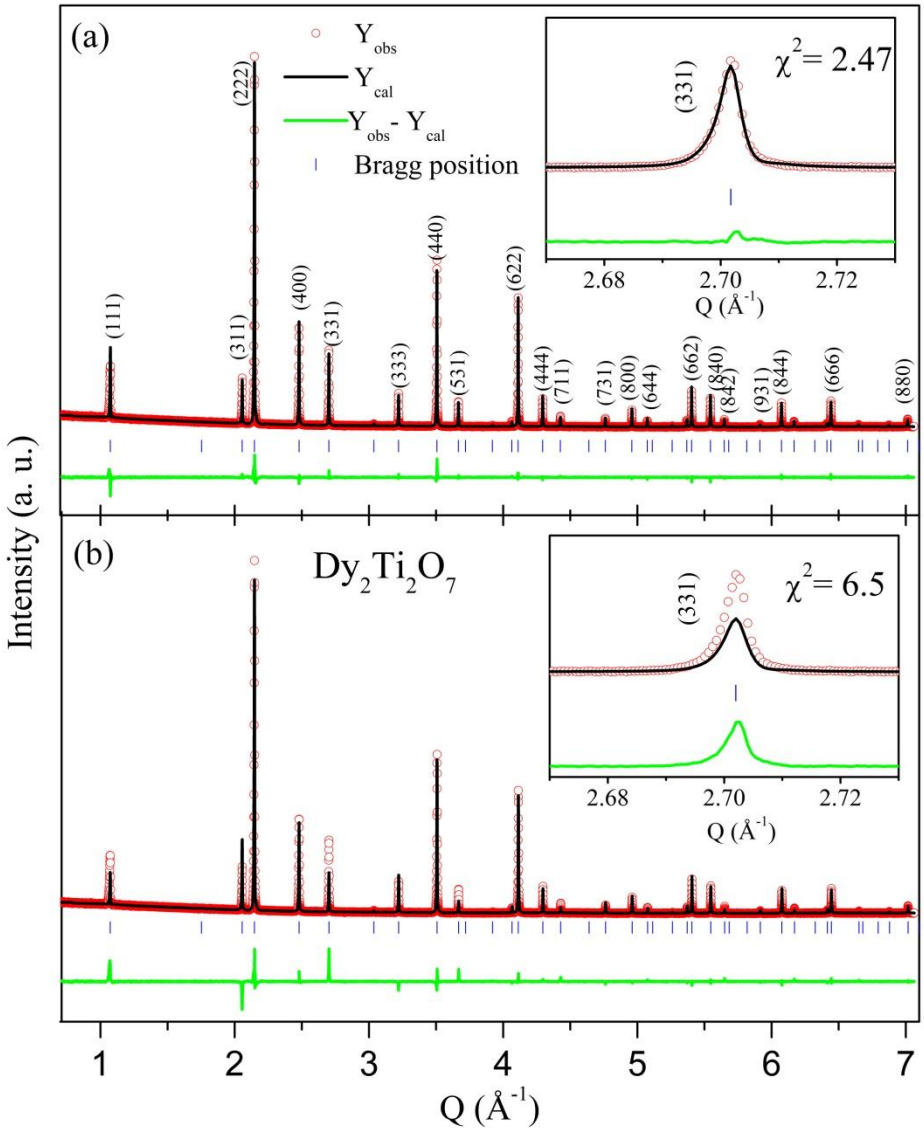

Figure 2.5: Rietveld refinement of the high-resolution x-ray diffraction patterns of $Dy_2Ti_2O_7$ by considering; (a) Dy^{3+} and Ti^{4+} at 16d and 16c crystallographic sites, respectively and (b) Dy^{3+} and Ti^{4+} at 16c and 16d crystallographic sites, respectively.

Table 2.2: Details of structural and fitting parameters as obtained from high-resolution x-ray diffraction. Compound, lattice constant, variable coordinate x in the 48f-site, R-factors (R_p, R_{wp} and R_e) and goodness of fit χ^2.

Compound	a (Å)	48f x, 0, 0	R_p	R_{wp}	R_e	χ^2
$Dy_2Ti_2O_7$	10.1270(1)	0.320(2)	21.9	15.4	9.82	2.47
$Ti_2Dy_2O_7$	10.1267(3)	0.419(1)	21.4	18.1	9.03	6.50

2.5 Conclusion

Pure phase sample of HTO, DTO and their doped derivatives has been synthesized by using conventional solid-state thermochemical reaction method as confirmed from the XRD measurement. Rietveld analysis of the XRD pattern of HTO and DTO further confirms the formation of pure phase cubic samples having space group $Fd\bar{3}m$ where atoms were situated at the sites intended for.